New perspectives on volcano monitoring in a tropical environment: continuous measurements of soil CO2 flux at Piton de la Fournaise (La Réunion Island, France)

Guillaume Boudoire, Andrea Di Muro, Marco Liuzzo, Valérie Ferrazzini, Aline Peltier, Stefano Gurrieri, Laurent Michon, Gaetano Giudice, Philippe Di Kowalski, Patrice Boissier

AGU PUBLICATIONS

Geophysical Research Letters

RESEARCH LETTER

10.1002/2017GL074237

Key Points:
- Robust correction of environmental influence on time series of soil CO_2 flux in tropical environment
- New procedure for continuous geochemical monitoring and early detection of volcano unrest, including in extreme tropical environment
- Complementarity between geophysical and geochemical networks to track and study fluid migration from mantle to crustal level

Supporting Information:
- Supporting Information S1
- Data Set S1

Correspondence to:
G. Boudoire,
guillaume.boudoire@gmail.com

Citation:
Boudoire, G., A. Di Muro, M. Liuzzo, V. Ferrazzini, A. Peltier, S. Gurrieri, L. Michon, G. Giudice, P. Kowalski, and P. Boissier (2017), New perspectives on volcano monitoring in a tropical environment: Continuous measurements of soil CO_2 flux at Piton de la Fournaise (La Réunion Island, France), *Geophys. Res. Lett.*, *44*, 8244–8253, doi:10.1002/2017GL074237.

Received 25 OCT 2016
Accepted 31 JUL 2017
Accepted article online 3 AUG 2017
Published online 19 AUG 2017

New perspectives on volcano monitoring in a tropical environment: Continuous measurements of soil CO_2 flux at Piton de la Fournaise (La Réunion Island, France)

G. Boudoire[1,2], A. Di Muro[2], M. Liuzzo[3], V. Ferrazzini[2], A. Peltier[2], S. Gurrieri[3], L. Michon[1], G. Giudice[3], P. Kowalski[2], and P. Boissier[2]

[1]Laboratoire Géosciences Réunion, Université de La Réunion, Institut de Physique du Globe de Paris (IPGP), Sorbonne Paris-Cité, UMR 7154 CNRS, Saint-Denis, France, [2]Observatoire Volcanologique du Piton de la Fournaise (OVPF), Institut de Physique du Globe de Paris (IPGP), Sorbonne Paris-Cité, UMR 7154 CNRS, Université Paris Diderot, CNRS, La Plaine des Cafres, France, [3]Istituto Nazionale di Geofisica e Vulcanologia, Palermo, Italy

Abstract Detecting renewal of volcanic activity is a challenging task and even more difficult in tropical settings. Continuous measurements of soil CO_2 flux were carried out at the Piton de la Fournaise volcano during 2013–2016. Since this site is in the tropics, periods of heavy rainfall are in the norm. Measurements covered volcanic unrest after a hiatus of 3.5 years. We find that while temperature has the strongest effect, extreme rainfall causes short-term noise. When corrected and filtered from the environmental influence, soil CO_2 time series permit to detect a major deep magmatic event during March–April 2014, 3 months before the first eruption of the new activity phase. Correlation with geophysical data sets allows timing of further stages of upward fluid ascent. Our study validates soil CO_2 flux monitoring in tropical environments as a valuable tool to monitor magma transfer and to enhance understanding of volcano unrest down to the lithospheric mantle.

1. Introduction

Many of the world's active volcanoes are set in the tropics, and their eruptions have the biggest impact on climate [*Shindell et al.*, 2004; *Fischer et al.*, 2007; *Vernier et al.*, 2011; *Vidal et al.*, 2016]. Monitoring these volcanoes is challenging due to dense vegetation and extreme weather conditions [*Pinel et al.*, 2011; *Ebmeier et al.*, 2013]. Moreover, most of them are located in developing countries and require the deployment of reliable low-cost monitoring tools answering to major socioeconomic issues [*Tilling*, 2008].

Diffuse soil degassing is an important component of the gas budget of an active volcano [*Allard et al.*, 1991; *Chiodini et al.*, 1998; *Diliberto et al.*, 2002; *Granieri et al.*, 2003; *Dionis et al.*, 2015]. The low solubility of carbon dioxide (CO_2) in magma and the high mobility of exsolved gases allow tracking magma transfer [*Giammanco et al.*, 1995, 2010; *Papale*, 1999; *Granieri et al.*, 2006; *Papale et al.*, 2006]. As a result, inputs of deep magmatic fluids have been clearly detected in the time evolution of soil CO_2 flux in various volcanic systems [*Hernandez et al.*, 2001; *Brusca et al.*, 2004; *Liuzzo et al.*, 2013].

Piton de la Fournaise (PdF) is one of the world's most active basaltic volcanoes. The island, close to the Tropic of Capricorn, has a tropical climate with a cold dry season (May–October) and a warm wet season (November–April) and experiences extreme rainfall events. The weak summit gas emissions have challenged geochemical monitoring to date [*Di Muro et al.*, 2016a]. Recent studies have highlighted the presence of high soil CO_2 flux on the volcano flanks during quiescence phases [*Liuzzo et al.*, 2015]. We here present results obtained from two sites where hourly measurements of soil CO_2 flux were performed during 3 years, overlapping the volcano reawakening. Raw, corrected, and filtered data allowed us to distinguish both the environmental and volcanic influences on the geochemical signal. Our study opens new perspectives for volcano monitoring in the tropics, even in weak degassing systems. It also emphasizes the link between geochemical and geophysical monitoring for early warning.

2. The Piton de la Fournaise Volcano

2.1. Piton de la Fournaise Plumbing System

Activity at PdF is fed by a shallow system that is linked to a deeper set of magma ponding zones hosting variably evolved and degassed melts [*Battaglia et al.*, 2005; *Peltier et al.*, 2009; *Di Muro et al.*, 2014, 2016a, 2016b].

Only small volumes of magma have been identified above sea level (asl) below the summit cone [*Peltier et al.*, 2010; *Di Muro et al.*, 2014]. Aseismic zones located between 0 and 1.5 km below sea level (bsl) could represent the main shallow reservoir [*Nercessian et al.*, 1996; *Peltier et al.*, 2009; *Prôno et al.*, 2009; *Lengliné et al.*, 2016]. An additional aseismic level between 7 and 11 km bsl [*Battaglia et al.*, 2005; *Michon et al.*, 2015] may constitute an intermediate storage zone that transfers magma into the shallow plumbing system [*Battaglia et al.*, 2005; *Peltier et al.*, 2009]. The deepest (>11 km bsl) zone of magma storage is known only in part and is presumably shifted to the western flank of the volcano [*Liuzzo et al.*, 2015; *Michon et al.*, 2015].

2.2. Piton de la Fournaise Recent Activity

Since 1930, Piton de la Fournaise has experienced an average of one eruption per year, interrupted by quiescent periods spanning 3 to 6 years [*Peltier et al.*, 2009; *Roult et al.*, 2012]. The 41 month long hiatus from 2011 to 2014 was marked by a continuous edifice deflation, low seismic activity, and low-temperature fumarolic emissions (C-S poor and H_2O rich) [*Peltier et al.*, 2016]. After only 11 days of weak inflation, the activity renewed in 20–21 June 2014. This marked the beginning of edifice inflation, increase in seismicity, and enrichment in C-S of gas emissions [*Peltier et al.*, 2016]. After a second eruption in February 2015, the unrest quickly ensued: since April 2015, seismic hypocenters moved from 7.5 to 2 km bsl, inflation rate increased, and CO_2 enrichment in summit fumaroles was detected [*Lengliné et al.*, 2016; *Peltier et al.*, 2016]. Shallow seismic events located 1.5–2.5 km bsl were recorded again the week before the May, July, and August–October 2015 eruptions [*Lengliné et al.*, 2016]. The August–October eruption was immediately followed by unusual deep seismicity (up to 7.5 km bsl). Only a few days of acceleration of the inflation and intensification of the shallow seismicity anticipated a new eruption in May 2016.

3. Methods

Soil CO_2 fluxes were acquired by the Observatoire Volcanologique du Piton de la Fournaise/Institut de Physique du Globe de Paris (OVPF/IPGP) during 3 years at two permanent stations (PCRN and PNRN) designed and assembled by the Istituto Nazionale di Geofisica e Vulcanologia (INGV) Sezione di Palermo [*Gurrieri et al.*, 2008]. Both stations were installed on the western flank of the volcano, 14 km from the central cone (Figure 1), in a sector known for its deep seismicity (>11 km bsl) and high soil CO_2 fluxes [*Liuzzo et al.*, 2015; *Michon et al.*, 2015]. PCRN (1560 m asl) was installed in the OVPF garden in 2012 and has continuously been functioning since August 2013. PNRN (1050 m asl) was set below the National Park building in 2013 and has provided continuous measurements since October 2014. The stations are regularly checked and cleared of vegetation.

Soil CO_2 flux measurements were made hourly, following the dynamic concentration method of *Gurrieri and Valenza* [1988]: a 50 cm long probe was inserted into the soil and connected by a Teflon pipe to a Gascard NG dual-wavelength nondispersive infrared gas analyzer (CO_2 gas measurement range 0–10%). The molar fraction of CO_2 is measured in a soil-air gas mixture pumped at 0.8 L/min and are automatically corrected for temperature and pressure effects on gas molecular density. Recorded values of soil CO_2 molar fraction fell in the linear working range of the IR sensors used (Table S1 in the supporting information). The soil CO_2 flux is derived from the soil CO_2 molar fraction by the following relation:

$$FCO_2 = \left(32\text{–}5.8\ k^{0.24}\right) C_d + 6.3\ k^{0.6}\ C_d{}^3$$

where ΦCO_2 is the soil CO_2 flux (g m^{-2} d^{-1}), C_d the soil CO_2 concentrations in molar fraction, and k is the soil permeability coefficient (μm^2) fixed here at 35 in accordance with previous studies on PdF [*Liuzzo et al.*, 2015, and references therein]. At PCRN, average soil CO_2 flux was 130 ± 45 g m^{-2} d^{-1} (full range from 6 to 224 g m^{-2} d^{-1}). At PNRN, average soil CO_2 flux was lower (12 ± 1 g m^{-2} d^{-1}; full range from 10 to 18 g m^{-2} d^{-1}). Spurious data related to rare anomalous electronic interference were removed from the data sets. Short gaps (<9 days and in 80% of cases <1 day) related to instrumental breakdown were filled by linear interpolation [*Liuzzo et al.*, 2013] (2% and 4% of the whole data set for PCRN and PNRN, respectively). Longer gaps (>25 days) were left as missing values.

Air temperature, pressure, relative humidity, case temperature, wind speed, and direction and rainfall were measured by an on-site meteorological station; soil temperature at 10 cm depth near PCRN was provided by Météo France. Rainfall data were compared or integrated with Météo France data to correct for local site effects. Tide gauge variations were provided by REFMAR. Soil CO_2 flux time series were correlated with eruptive activity, geodetic, and seismic data. Seismic data were divided into three categories: central

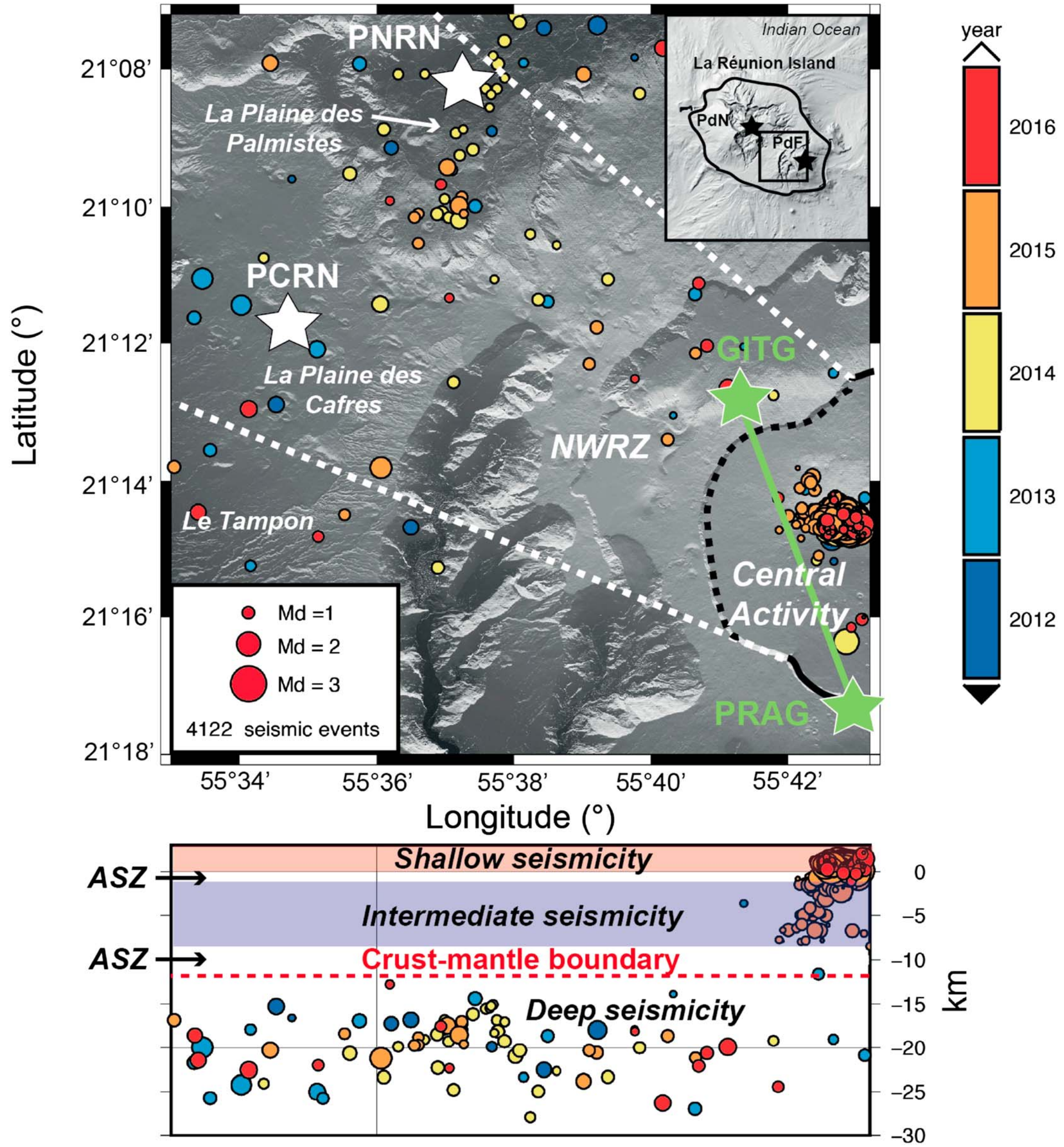

Figure 1. Context map of the study made with the Generic Mapping Tools software [*Wessel and Smith*, 1998]. Inset shows the location of Piton de la Fournaise (PdF) and Piton des Neiges (PdN) volcanoes on La Réunion Island. PCRN and PNRN are the two permanent stations (white stars) measuring soil CO_2 molar fractions discussed in this paper. Baseline (green line) is the line length between GITG and PRAG GNSS stations (green stars), whose elongation tracks PdF deformation. Volcano-tectonic earthquakes recorded between 2012 and 2016 are reported by colored dots. Note the occurrence of (1) deep seismicity at mantle depth (>11 km bsl) below the western volcano flank and the (2) intermediate (9–2 km bsl) and (3) shallow seismicity (0–2 km asl) below the summit cone. Two aseismic zones (ASZ) separate these three groups of seismic events [*Nercessian et al.*, 1996; *Lengliné et al.*, 2016].

shallow (0–2 km asl), central intermediate (2–9 km bsl), and deep (>11 km bsl). At Piton de la Fournaise, geophysical signals are weak, all seismic events have a magnitude <2, and the amplitude of the GITG-PRAG (GNSS stations) baseline variation did not exceed 6 cm during the investigated period (modeling an inflation source shallower than 2 km bsl) [*Peltier et al.*, 2016].

4. Results

4.1. Correcting Soil CO_2 Flux for Environmental Influence

Obtaining information about a volcanic system from soil CO_2 flux time series requires first to identify the influence of environmental parameters [*Viveiros et al.*, 2008; *Giammanco et al.*, 2010; *Liuzzo et al.*, 2013].

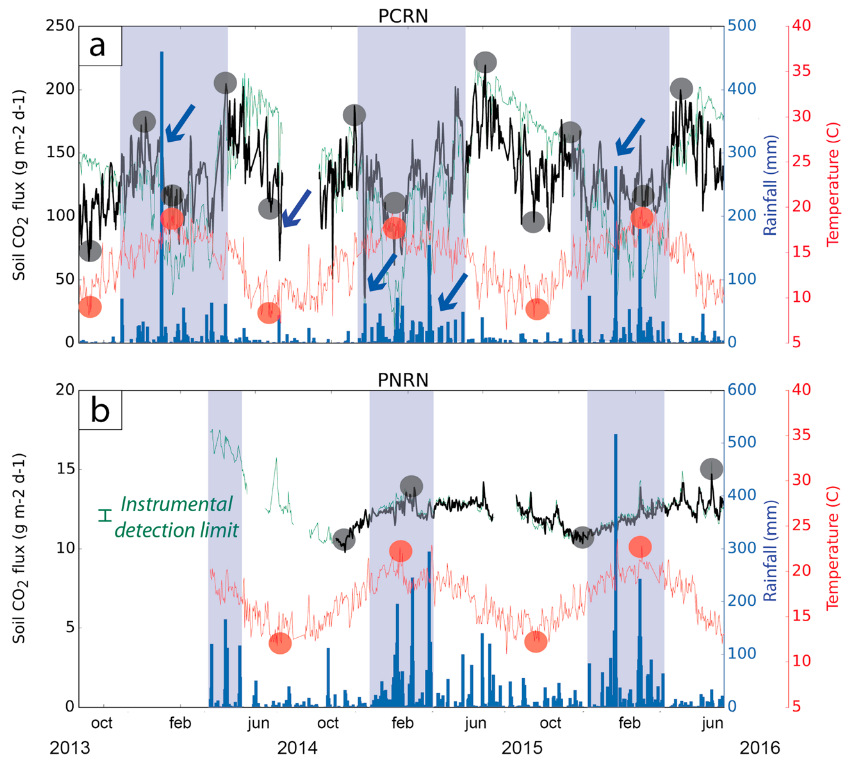

Figure 2. Raw soil CO_2 fluxes (green lines) and data corrected by multiple linear regression (black lines) at (a) PCRN (22 August 2013 to 22 June 2016) and (b) PNRN (21 March 2014 to 22 June 2016). Red lines show air temperature at each site. Shaded black and red filled circles represent extreme soil CO_2 fluxes and air temperature values, respectively, determined on 15 days moving average. Blue shaded areas represent rainy seasons defined on cumulative plots. Blue histograms the daily rainfall at each site. Short-lived soil CO_2 flux decreases related to rain events are highlighted by blue arrows.

To do this, we correlated soil CO_2 flux time series with all recorded environmental parameters. We used daily averaged values, to remove the influence of daily cycles of pressure and temperature [*Di Martino et al.*, 2013]. We found that daily average temperature and pressure exert the largest influence on soil CO_2 flux, without time delay (Table S2), as observed in other volcanic systems [*Giammanco et al.*, 2010; *Liuzzo et al.*, 2013]. Strong multicollinearity between these parameters (Table S3) permits the application of a simple linear regression with air temperature. Only a slight difference is found when using distinct temperature sensors, ($r^2 = 0.61$ with Météo France sensor, instead of 0.58 with INGV sensor at PCRN station). This air temperature correction, based on Météo France data, reduces the noisy environmental contributions to 5% of the signal for PCRN (Figure 2a) and 12% for PNRN (Figure 2b). Wind speed plays a secondary order role only at PNRN ($r^2 = 0.07$; Table S2), as observed on other volcanoes [*Viveiros et al.*, 2008; *Carapezza et al.*, 2009]. Analysis of the wind speed influence reveals that soil CO_2 flux is slightly more affected when wind exceeds 0.1 m s^{-1} ($r^2 = 0.18$; determined by graphical approach [*Sinclair*, 1974]). Thus, a second linear regression was applied to lower this effect to an environmental contribution <3%.

4.2. Filtering Soil CO_2 Flux for Seasonal Effects

Long-term seasonal effects involving a long-period component (between 300 and 400 days) may also influence soil CO_2 flux [*Liuzzo et al.*, 2013]. This periodic variation is strongly related to air temperature variation (Figures 2a and 2b; periodicity of 270–380 days). At PCRN, soil CO_2 flux maxima and minima were recorded during temperature extrema events (Figure 2a). Conversely, at PNRN, where fluxes are much lower than at PCRN, weak seasonal effects shifted with respect to temperature may occur (Figure 2b). To filter this seasonal effect, we removed the main component between 270 and 380 days by fast Fourier transform analysis (FFT). Admittedly, longer time series are required to better study this potential seasonal effect.

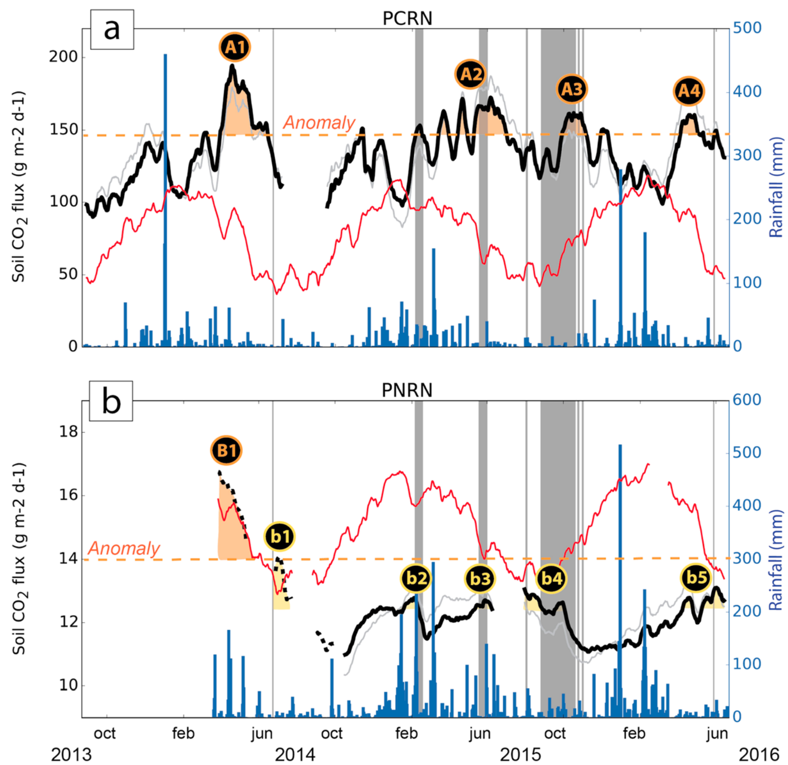

Figure 3. Comparison between 15 day moving averages of soil CO_2 fluxes corrected for (i) the effect of temperature (red lines) and wind (gray lines) by linear regression and (ii) by FFT filtering on the 1 year component (black line) for (a) PCRN and (b) PNRN. Gray shaded areas are eruptive periods, and blue histograms are daily rainfall at each site. *A*1, *A*2, *A*3, *A*4 for PCRN and *B*1 for PNRN account for the main soil CO_2 flux anomalies (orange shaded areas). Letters *b*1, *b*2, *b*3, *b*4, and *b*5 for PNRN mark secondary soil CO_2 flux anomalies below the current threshold definition (yellow shaded areas).

Rainfall is known to have a short-term effect on soil CO_2 flux by inducing permeability changes [*Granieri et al.*, 2003; *Liuzzo et al.*, 2013]. Filtering the signals by the annual component related to temperature seasonality determines a further reduction on the potential influence of rainy seasons. Nevertheless, to take into account the rainy tropical environment of La Réunion, we performed a careful analysis of the influence of rain seasonality and strong rain events on corrected soil CO_2 flux (Figure 2). We found no significant correlation between rainfall and soil CO_2 flux ($r^2 < 0.01$ for both stations). At PCRN, extreme rainfall events induced short-lived decreases in soil CO_2 flux, but none exceeded a few days (Figure 2a; cf. blue arrows). Similar high-frequency noise in soil CO_2 flux produced by rain has been described in other volcanic systems [*Liuzzo et al.*, 2013, and references therein]. This effect is particularly negligible for the PNRN station, which is set up in dry conditions (Figure 2b). In order to flatten the noise related to rain events, we applied a 15 day long moving average to the signal. This smoothing length was selected in order to (i) minimize tidal effects (12.5 h and 14 days full cycles) [*Roult et al.*, 2012] and (ii) reduce the loss of soil CO_2 flux signal (Figures 3a and 3b).

4.3. Soil CO_2 Flux Anomalies

In order to identify anomalies in time series, soil CO_2 flux populations were characterized using both the Sinclair graphical approach [*Sinclair*, 1974] and the maximum-likelihood method [*Elio et al.*, 2016]. Both methods produce similar results (Table S4). The advantage of the last one is that it provides thresholds and an estimation of the contribution of the different populations to a value independent of the operator choice. Two and three populations are found in the PCRN and PNRN data sets, respectively (Table S4). Population 1 ($>$145 g m^{-2} d^{-1} and $>$14 g m^{-2} d^{-1} at PCRN and PNRN, respectively) is considered as representative of anomalous values (in orange in Figure 3). Additionally, at PNRN, we identified high-frequency small peaks belonging to an intermediate Population 2 ($>$12.3 g m^{-2} d^{-1} on average; in yellow in Figure 3b).

PCRN station showed the stronger positive anomaly (*A*1; Figure 3a). It began to be evident on 31 March 2014 and reached its maximum on 19 April 2014. Other anomalies (*A*2, *A*3, and *A*4) have lower magnitudes. *A*2 began on 15 March 2015 and accelerated on 15 April 2015 to reach its maxima on 22 April and 7 June. *A*3 started on 28 September 2015 and culminated on 16 October 2015. *A*4 began on 4 April 2016 and reached its maxima on 27 April 2016. It is worth noting that most of these anomalies occurred at the end of the rainy season and eruptive events tend to increase in frequency afterward. Such a relationship was also found by *Roult et al*. [2012], who suggested a seasonal effect at Piton de la Fournaise with activity distribution (1985–2010 period) being related to the annual hydrological cycle.

At PNRN, the only strong positive anomaly (*B*1*)* occurred in March–April 2014 or even before (no data) and its timing overlaps with that of the main anomaly (*A*1*)* of PCRN (Figure 3b). Five lower magnitude anomalies can be identified: *b*1 (approximately 4 July 2014), *b*2 (approximately 5 February 2015), *b*3 (approximately 29 May 2015), *b*4 (approximately 13 August and 30 September 2015), and *b*5 (approximately 20 April and 2 June 2016). Despite the fact that the PNRN anomalies were short lived and of low magnitude, it is interesting to note a broad synchronicity with the eruptive events (Figure 3b). However, we emphasize that their meaning requires a longer temporal series in order to correct the long-term environmental trend.

5. Discussion

5.1. Correlation With Geophysical Data

Multiparametric monitoring networks have demonstrated the efficacy of combining continuous geochemical and geophysical measurements to identify short- and long-term precursors of volcanic activity [*Wright and Klein*, 2008; *Aiuppa et al.*, 2010; *Patanè et al.*, 2013; *Peltier et al.*, 2016].

At PCRN, we found that soil CO_2 flux anomalies (*A*1, *A*2, *A*3, and *A*4 in Figure 4a) are coeval with periods of enhanced deep (mantellic) seismic activity below the western flank of the volcano (*S*1, *S*2, *S*3, and *S4* in Figure 4b). The largest soil CO_2 flux anomaly event in March–May 2014 (*A*1) is synchronous with the most intense seismic period below the western flank (*S*1). By contrast, soil CO_2 flux is mostly anticorrelated with the increase in the shallow seismicity below the central area (red arrows in Figure 4a). During the same period, the distal GITG-PRAG baseline shows an alternation of step plateaus (horizontal dashed lines in Figure 4c) and elongation phases [*Peltier et al.*, 2016]. We found that the soil CO_2 flux was also broadly anticorrelated with inflation phases (red arrows in Figure 4a; Figure S1). Only two periods displayed a positive correlation between all the geochemical and geophysical records in the central area (blue arrows in Figure 4a): in April 2015 (*A*2) and in October 2015 (*A*3). In both cases, unusual high levels of seismicity were recorded in the deepest part of the central plumbing system (7.5 km bsl; Figure 4b). Note that the short inflation phase in January 2016 (green arrow in Figure 4c) is decorrelated from the soil CO_2 flux and from the seismicity. It is also the only phase in the whole investigated period not immediately followed by an eruptive phase.

At PNRN, the largest soil CO_2 anomaly (*B*1) occurred before the June 2014 eruption, concomitant with the main positive anomaly (*A*1) at PCRN and with deep seismicity below the western flank. Noteworthy, deep seismicity was located below La Plaine des Palmistes where the station is located (Figure 1). Soil CO_2 flux began to decrease just before the June 2014 eruption and does not record a similar anomaly in the following period. Interestingly, the low-magnitude *b*1, *b*2, *b*3, *b*4, and *b*5 anomalies are correlated with peaks in distal volcano inflation (cross correlation = 0.92; Figure S2). However, this correlation needs further investigations on larger data sets for confirmation.

5.2. Reactivation of Piton de la Fournaise: The 2014–2016 Period

The geochemical and geophysical time series acquired since mid-2013 provide new constraints on magmatic processes occurring at the transition between quiescence and eruptive activity at Piton de la Fournaise. Based on the comparison between the main soil CO_2 flux anomalies detected and the geophysical signals, we identify two distinct cases ((1) and (2) in Figure 4):

1. The first case is soil CO_2 flux anomalies (*A*1-*B*1 and *A*4 in Figure 4a) concomitant only with swarms of deep seismic events at lithospheric mantle level, below the western flank of the volcano.

   The main soil CO_2 flux anomaly detected by both stations (*A*1-*B*1) on the volcano flanks marked the reactivation of the volcano after a 41 month quiescent period and preceded by 3 months the June 2014

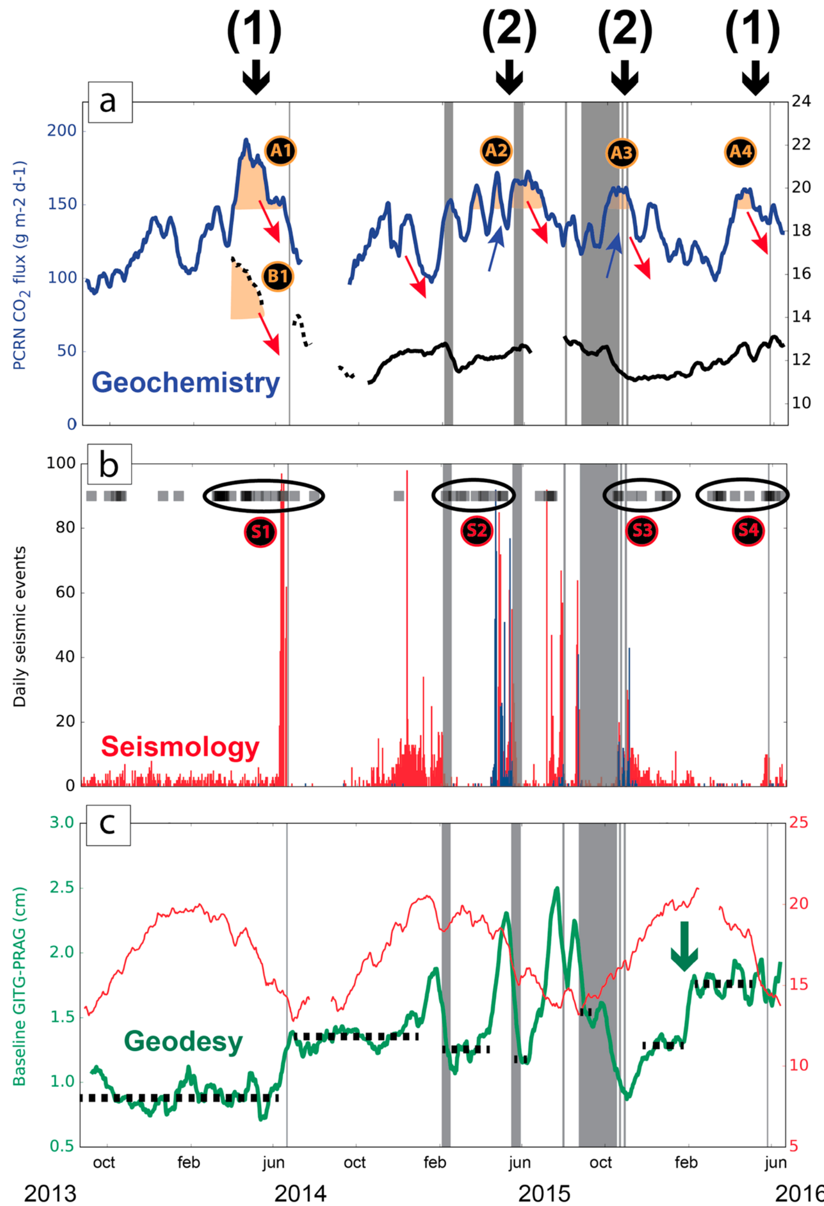

Figure 4. Comparison between 15 day moving averages of (a) soil CO_2 fluxes for PCRN (blue line) and PNRN stations (black line) with the main identified anomalies (see Figure 3). (b) Deep (number of events increasing from gray to black boxes), intermediate (blue histograms), and shallow seismic events (red histograms). (c) Distance change along the distal GITG-PRAG baseline (green line). In red, air temperature at PNRN. The green arrow highlights inflation phase decorrelated from other geophysical and geochemical records. All reported geodetical and geochemical peaks are significantly larger than the detection thresholds. Red arrows point to anticorrelation (soil CO_2 flux decrease, inflation, and seismicity increase) between soil CO_2 flux and geophysical signals. Blue arrows represent positive correlations. Correlations between all geophysical and geochemical records suggest two distinct behaviors (i.e., (1) and (2)) during the investigated periods (see text for explanations).

summit eruption. A weaker amplitude case started on 4 April 2016, when a new soil CO_2 flux anomaly was detected at PCRN (*A4*).

Importantly, for these deep processes, geophysical records tracking central shallow processes show little if anything. Central shallow seismicity and inflation rate only started to increase when soil CO_2 flux decreased. Such anticorrelations have already been observed on Mount Etna (Sicily, Italy), where they have been attributed to fluid migration from the deepest part of the plumbing system toward the central, shallowest part of the system [*Liuzzo et al.*, 2013; *Cannata et al.*, 2015]. We state that this conceptual model may be also relevant at Piton de la Fournaise.

2. The second case is soil CO_2 flux anomalies (*A*2 and *A*3 in Figure 4a) correlated with edifice inflation and with the appearance of unusually high levels of seismicity in the deepest part of the central plumbing system (7.5 km bsl).

   This case was observed in April 2015 (*A*2), when soil CO_2 fluxes attained high values on 15 April 2015 at PCRN. Acceleration of ground deformation started on 13 April and coincided with migration of seismic hypocenters below the summit crater on 16 April (between 7.5 and 1.5 km bsl) [*Lengliné et al.*, 2016]. Geochemical and geophysical precursors heralded the closely spaced May, July, and August–October 2015 eruptions. This scenario was also observed during the long-lived August–October 2015 eruption, marked by soil CO_2 flux increasing in September 2015 (*A*3). Once again, this anomaly was synchronous with renewal of inflation and the reappearance of unusual seismicity in the deepest roots of the central plumbing system (i.e., 7.5 km bsl). This phase was also marked by a change in the composition of the emitted magma and an increase in magma and gas discharge rate [*Di Muro et al.*, 2016b; *Coppola et al.*, 2017].

   Such correlations would suggest that deep fluid migration was involved into the reactivation of the whole plumbing system, producing a synchronous increase in soil CO_2 flux, CO_2 enrichment in summit fumaroles, acceleration of central seismicity, and inflation [*Lengliné et al.*, 2016; *Peltier et al.*, 2016].

6. Conclusion

Detecting the beginning of volcano unrest is challenging, especially in tropical settings. Analysis of a 3 year long time series of soil CO_2 flux at two stations located on the western flank of the Piton de la Fournaise volcano successfully filtered the short-term and seasonal influences of air temperature, wind, and rain. The corrected and filtered geochemical signal revealed (i) several positive anomalies above background and (ii) periods of strong decrease in soil CO_2 flux. Both stations recorded a strong increase in soil CO_2 flux in March–April 2014. This anomaly was synchronous with the main swarm of deep (mantellic) seismic events below the western flank and preceded by 3 months, the reactivation of the volcano after a 41 month rest period. Soil CO_2 flux declined just before the first eruption in June 2014. During 2015, farther but weaker anomalies were recorded at the site with higher soil CO_2 fluxes (PCRN), synchronous either with the deep seismicity below the western flank or with the reactivation of the whole central plumbing system (seismicity and edifice inflation). Decrease of soil CO_2 flux on the western flank appeared mainly anticorrelated with accelerations of geophysical records associated with shallow processes.

Continuous measurement of soil CO_2 flux on the western volcano flank, coupled with monitoring of subtle edifice inflation at increasing distance from the central cone, and time and space evolution of microseismic events over the whole edifice allowed us to track fluid transfers at the depth of over 30 km. Merging of soil degassing time series with data from geophysical networks opens exciting new prospects for capturing volcanic unrest in extreme tropical environments.

Acknowledgments

A.L. Rizzo and C. Federico (INGV) and P. Allard (IPGP) are gratefully acknowledged for constructive discussions. We thank A. Harris (LMV) for performing an informal review of the manuscript and F. Di Muro for proofreading. Météo France and REFMAR (http://data.shom.fr) are acknowledged for providing data. Tables S1–S4 and Figures S1–S3 are available as supporting information. The GNSS, seismic, and gas data used in this paper were collected by the OVPF/IPGP. All data used in this study are available in an Excel file as supporting information. Part of this work has been funded by Université de La Réunion and by the ANR STRAP (ANR-14-CE03-0004). This is IPGP contribution number 3872.

References

Aiuppa, A., et al. (2010), Patterns in the recent 2007–2008 activity of Mount Etna volcano investigated by integrated geophysical and geochemical observations, *Geochem. Geophys. Geosyst.*, *11*, Q09008, doi:10.1029/2010GC003168.

Allard, P., et al. (1991), Eruptive and diffuse emissions of CO_2 from Mount Etna, *Nature*, *351*, 387–391, doi:10.1038/351387a0.

Battaglia, J., V. Ferrazzini, T. Staudacher, K. Aki, and J. L. Cheminée (2005), Pre-eruptive migration of earthquakes at the Piton de la Fournaise volcano (Réunion Island), *Geophys. J. Int.*, *161*, 549–558, doi:10.1111/j.1365-246X.2005.02606.x.

Brusca, L., S. Inguaggiato, M. Longo, P. Madonia, and R. Maugeri (2004), The 2002–2003 eruption of Stromboli (Italy): Evaluation of the volcanic activity by means of continuous monitoring of soil temperature, CO_2 flux, and meteorological parameters, *Geochem. Geophys. Geosyst.*, *5*, Q12001, doi:10.1029/2004GC000732.

Cannata, A., G. Spedalieri, B. Behncke, F. Cannavò, G. Di Grazia, S. Gambino, S. Gresta, S. Gurrieri, M. Liuzzo, and M. Palano (2015), Pressurization and depressurization phases inside the plumbing system of Mount Etna volcano: Evidence from a multiparametric approach, *J. Geophys. Res. Solid Earth*, *120*, 5965–5982, doi:10.1002/2015JB012227.

Carapezza, M. L., T. Ricci, M. Ranaldi, and L. Tarchini (2009), Active degassing structures of Stromboli and variations in diffuse CO_2 output related to the volcanic activity, *J. Volcanol. Geotherm. Res.*, *182*, 231–245, doi:10.1016/j.jvolgeores.2008.08.006.

Coppola, D., et al. (2017), Shallow system rejuvenation and magma discharge trends at Piton de la Fournaise volcano (La Réunion Island), *Earth Planet. Sci. Lett.*, *463*, 13–24.

Chiodini, G., R. Cioni, M. Guidi, B. Raco, and L. Marini (1998), Soil CO_2 flux measurements in volcanic and geothermal areas, *Appl. Geochem.*, *13*, 543–552.

Diliberto, I. S., S. Gurrieri, and M. Valenza (2002), Relationships between diffuse CO_2 emissions and volcanic activity on the island of Vulcano (Aeolian Island, Italy) during the period 1984–1994, *Bull. Volcanol.*, *64*, 219–228.

Di Martino, R. M. R., M. Camarda, S. Gurrieri, and M. Valenza (2013), Continuous monitoring of hydrogen and carbon dioxide at Mt Etna, *Chem. Geol.*, *357*, 41–51, doi:10.1016/j.chemgeo.2013.08.023.

Di Muro, A., N. Métrich, D. Vergani, M. Rosi, P. Armienti, T. Fougeroux, E. Deloule, I. Arienzo, and L. Civetta (2014), The shallow plumbing system of Piton de la Fournaise volcano (La Réunion Island, Indian Ocean) revealed by the major 2007 caldera-forming eruption, *J. Petrol.*, *55*, 1287–1315.

Di Muro, A., N. Métrich, P. Allard, A. Aiuppa, M. Burton, B. Galle, and T. Staudacher (2016a), Magma degassing at Piton de la Fournaise volcano, in *Active Volcanoes of the Southwest Indian Ocean: Piton de la Fournaise and Karthala*, *Active Volcanoes of the World*, pp. 203–222, edited by P. Bachèlery et al., Springer, Berlin.

Di Muro, A., et al. (2016b), Eruption and degassing dynamics of the major August 2015 Piton de la Fournaise eruption, EGU General Assembly, Vienna.

Dionis, S. M., et al. (2015), Diffuse volcanic gas emission and thermal energy release from the summit crater of Pico do Fogo, Cape Verde, *Bull. Volcanol.*, *77*, 2, doi:10.1007/s00445-014-0897-4.

Ebmeier, S. K., J. Biggs, T. A. Mather, and F. Amelung (2013), Applicability of InSAR to tropical volcanoes: Insights from Central America, *Geol. Soc. Lond., Spec. Publ.*, *380*(1), 15–37.

Elio, J., M. F. Ortega, B. Nisi, L. F. Mazadiego, O. Vaselli, J. Caballero, and E. Chacon (2016), A multi-statistical approach for estimating the total output of CO_2 from diffusive soil degassing by the accumulation chamber method, *Int. J. Greenhouse Gas Control*, *47*, 351–363.

Fischer, E. M., J. Luterbacher, E. Zorita, S. F. B. Tett, C. Casty, and H. Wanner (2007), European climate response to tropical volcanic eruptions over the last half millennium, *Geophys. Res. Lett.*, *34*, L05707, doi:10.1029/2006GL027992.

Giammanco, S., S. Gurrieri, and M. Valenza (1995), Soil CO_2 degassing on Mt. Etna (Sicily) during the period 1989–1993: Discrimination between climatic and volcanic influences, *Bull. Volcanol.*, *57*, 52–60.

Giammanco, S., F. Bellotti, G. Groppelli, and A. Pinton (2010), Statistical analysis reveals spatial and temporal anomalies of soil CO_2 efflux on Mount Etna volcano (Italy), *J. Volcanol. Geotherm. Res.*, *194*, 1–14, doi:10.1016/j.jvolgeores.2010.04.006.

Granieri, D., G. Chiodini, W. Marzocchi, and R. Avino (2003), Continuous monitoring of CO_2 soil diffuse degassing at Phlegraean Fields (Italy): Influence of environmental and volcanic parameters, *Earth Planet. Sci. Lett.*, *212*, 167–179, doi:10.1016/S0012-821X(03)00232-2.

Granieri, D., M. L. Carapezza, G. Chiodini, R. Avino, S. Caliro, M. Ranaldi, T. Ricci, and L. Tarchini (2006), Correlated increase in CO_2 fumarolic content and diffuse emission from La Fossa crater (Vulcano, Italy): Evidence of volcanic unrest or increasing gas release from a stationary deep magma body?, *Geophys. Res. Lett.*, *33*, L13316, doi:10.1029/2006GL026460.

Gurrieri, S., and M. Valenza (1988), Gas transport in natural porous mediums: A method for measuring CO_2 flows from the ground in volcanic and geothermal areas, *Rend. Soc. Ital. Mineral. Petrol.*, *43*, 1151–1158.

Gurrieri, S., M. Liuzzo, and G. Giudice (2008), Continuous monitoring of soil CO_2 flux on Mt. Etna: The 2004–2005 eruption and the role of regional tectonics and volcano tectonics, *J. Geophys. Res.*, *113*, B09206, doi:10.1029/2007JB005003.

Hernandez, P. A., K. Notsu, J. M. Salazar, T. Mori, G. Natale, H. Okada, G. Virgili, Y. Shimoike, M. Sato, and N. M. Perez (2001), Carbon dioxide degassing by advective flow from Usu volcano, Japan, *Science*, *292*, 83–86.

Lengliné, O., Z. Duputel, and V. Ferrazzini (2016), Uncovering the hidden signature of a magmatic recharge at Piton de la Fournaise volcano using small earthquakes, *Geophys. Res. Lett.*, *43*, 4255–4262, doi:10.1002/2016GL068383.

Liuzzo, M., S. Gurrieri, G. Giudice, and G. Giuffrida (2013), Ten years of soil CO_2 continuous monitoring on Mt. Etna: Exploring the relationship between processes of soil degassing and volcanic activity, *Geochem. Geophys. Geosyst.*, *14*, 2886–2899, doi:10.1002/ggge.20196.

Liuzzo, M., A. Di Muro, G. Giudice, L. Michon, V. Ferrazzini, and S. Gurrieri (2015), New evidence of CO_2 soil degassing anomalies on Piton de la Fournaise volcano and the link with volcano tectonic structures, *Geochem. Geophys. Geosyst.*, *16*, 4388–4404, doi:10.1002/2015GC006032.

Michon, L., V. Ferrazzini, A. Di Muro, N. Villeneuve, and V. Famin (2015), Rift zones and magma plumbing system of Piton de la Fournaise volcano: How do they differ from Hawaii and Etna, *J. Volcanol. Geotherm. Res.*, *303*, 112–129.

Nercessian, A., A. Hirn, J. C. Lépine, and M. Sapin (1996), Internal structure of Piton de la Fournaise volcano from seismic wave propagation and earthquake distribution, *J. Volcanol. Geotherm. Res.*, *70*(3–4), 123–143.

Papale, P. (1999), Modeling of the solubility of a two-component $H_2O + CO_2$ fluid in silicate liquids, *Am. Mineral.*, *84*, 477–492.

Papale, P., R. Moretti, and D. Barbato (2006), The compositional dependence of the saturation surface of $H_2O + CO_2$ fluids in silicate melts, *Chem. Geol.*, *229*, 78–95.

Patanè, D., et al. (2013), Insights into magma and fluid transfer at Mount Etna by a multiparametric approach: A model of the events leading to the 2011 eruptive cycle, *J. Geophys. Res. Solid Earth*, *118*, 3519–3539, doi:10.1002/jgrb.50248.

Peltier, A., P. Bachèlery, and T. Staudacher (2009), Magma transport and storage at Piton de la Fournaise (La Réunion) between 1972 and 2007: A review of geophysical and geochemical data, *J. Volcanol. Geotherm. Res.*, *184*, 93–108, doi:10.1016/j.jvolgeores.2008.12.008.

Peltier, A., T. Staudacher, and P. Bachèlery (2010), New behaviour of the Piton de la Fournaise volcano feeding system (La Réunion Island deduced from GPS data: Influence of the 2007 Dolomieu crater collapse), *J. Volcanol. Geotherm. Res.*, *192*, 48–56, doi:10.1016/j.jvolgeores.2010.02.007.

Peltier, A., F. Beauducel, N. Villeneuve, V. Ferrazzini, A. Di Muro, A. Aiuppa, A. Derrien, K. Jourde, and B. Taisne (2016), Deep fluid transfer evidenced by surface deformation during the 2014-2015 unrest at Piton de la Fournaise volcano, *J. Volcanol. Geotherm. Res.*, *321*, 140–148, doi:10.1016/j.jvolgeores.2016.04.031.

Pinel, V., A. Hooper, S. De la Cruz-Reyna, G. Reyes-Davila, M. P. Doin, and P. Bascou (2011), The challenging retrieval of the displacement field from InSAR data for andesitic stratovolcanoes: Case study of Popocatepetl and Colima Volcano, Mexico, *J. Volcanol. Geotherm. Res.*, *200*, 49–61, doi:10.1016/j.jvolgeores.2010.12.002.

Prôno, E., J. Battaglia, V. Monteiller, J. L. Got, and V. Ferrazzini (2009), P-wave velocity structure of Piton de la Fournaise volcano deduced from seismic data recorded between 1996 and 1999, *J. Volcanol. Geotherm. Res.*, *184*, 49–62, doi:10.1016/j.jvolgeores.2008.12.009.

Roult, G., A. Peltier, B. Taisne, T. Staudacher, V. Ferrazzini, A. Di Muro, and OVPF Team (2012), A new comprehensive classification of the Piton de la Fournaise activity spanning the 1985–2010 period. Search and analysis of short-term precursors from a broad-band seismological station, *J. Volcanol. Geotherm. Res.*, *241–242*, 78–104, doi:10.1016/j.jvolgeores.2012.06.012.

Shindell, D. T., G. A. Schmidt, M. E. Mann, and G. Faluvegi (2004), Dynamic winter climate response to large tropical volcanic eruptions since 1600, *J. Geophys. Res.*, *109*, D05104, doi:10.1029/2003JD004151.

Sinclair, A. J. (1974), Selection of threshold values in geochemical data using probability graphs, *J. Geochem. Explor.*, *3*, 129–149.

Tilling, R. I. (2008), The critical role of volcano monitoring in risk reduction, *Adv. Geosci.*, *14*, 3–11.

Vernier, J.-P., et al. (2011), Major influence of tropical volcanic eruptions on the stratospheric aerosol layer during the last decade, *Geophys. Res. Lett.*, *38*, L12807, doi:10.1029/2011GL047563.

10.1002/2017GL074237

Vidal, C. M., N. Metrich, J. C. Komorowski, I. Pratomo, A. Michel, N. Kartadinata, V. Robert, and F. Lavigne (2016), The 1257 Samalas eruption (Lombok, Indonesia): The single-greatest stratospheric gas release of the Common Era, *Sci. Rep.*, *6*, 34868, doi:10.1038/srep34868.

Viveiros, F., T. Ferreira, J. Cabral Vieira, C. Silva, and J. L. Gaspar (2008), Environmental influences on soil CO_2 degassing at Furnas and Fogo volcanoes (São Miguel Island, Azores archipelago), *J. Volcanol. Geotherm. Res.*, *177*, 883–893, doi:10.1016/j.jvolgeores.2008.07.005.

Wessel, P., and W. H. Smith (1998), New, improved version of generic mapping tools released, *Eos. Trans. AGU*, *79*(47), 579–579.

Wright, T. L., and F. W. Klein (2008), Dynamics of magma supply to Kilauea volcano, Hawaii: Integrating seismic, geodetic, and eruption data, in *Dynamics of Crustal Magma Transfer, Storage, and Differentiation*, *Spec. Publ*, edited by C. Annen and G. F. Zellmer, pp. 83–116, Geol. Soc., London.